Eur Biophys J (2008) 37:1133–1137
DOI 10.1007/s00249-007-0253-0

ORIGINAL PAPER

Oriented epitaxial growth of amyloid fibrils of the N27C mutant β25–35 peptide

Árpád Karsai · Ünige Murvai · Katalin Soós · Botond Penke · Miklós S. Z. Kellermayer

Received: 27 September 2007 / Revised: 7 December 2007 / Accepted: 13 December 2007 / Published online: 9 January 2008

Abstract Amyloid fibrils are present in the extracellular space of various tissues in neurodegenerative and protein misfolding diseases. Amyloid fibrils may be used in nanotechnology applications, because of their self-assembly properties and stability, if their growth and orientation can be controlled. Recently, we have shown that amyloid β25–35 (Aβ25–35) forms a highly oriented, K^+-dependent network on mica. Here, we analyzed the properties of Aβ25–35_N27C, the cysteine residue of which may be used for subsequent chemical modifications. We find that Aβ25–35_N27C forms epitaxially growing fibrils on mica, which evolve into a trigonally oriented branched network. The binding is apparently more sensitive to cation concentration than that of the wild-type peptide. By nanomanipulating Aβ25–35_N27C fibrils with a gold-coated AFM tip, we show that the sulfhydryl of Cys27 is reactive and accessible from the solution. The oriented network of Aβ25–35_N27C fibrils can therefore be specifically labeled and may be used for constructing nanobiotechnological devices.

Regional Biophysics Conference of the National Biophysical Societies of Austria, Croatia, Hungary, Italy, Serbia, and Slovenia.

Á. Karsai · Ü. Murvai · M. S. Z. Kellermayer (✉)
Department of Biophysics, Faculty of Medicine,
University of Pécs, Szigeti u. 12, H-7624 Pécs, Hungary
e-mail: miklos.kellermayer.jr@aok.pte.hu

K. Soós
Department of Medical Chemistry, University of Szeged,
Dóm tér 8, H-6720 Szeged, Hungary

B. Penke
Supramolecular and Nanostructured Materials Research Group
of the Hungarian Academy of Sciences, Dóm tér 8,
H-6720 Szeged, Hungary

Keywords Amyloid · Atomic force microscopy · Epitaxial growth · Nanoscale network · Sulfhydryl chemistry · β-sheet

Introduction

Amyloid fibrils are proteinaceous filaments, which, under in vivo conditions and in a variety of degenerative diseases, become deposited in the extracellular space of different tissues (Hardy and Selkoe 2002; Selkoe 2001; Selkoe 2003; Serpell 2000). Amyloid peptides have been suggested to self-assemble into specific nanostructures such as nanosensors and conductive nanowires (Gazit 2006; Hamada et al. 2004; Reches and Gazit 2003; Scheibel et al. 2003). A special advantage of amyloid peptides is that variants suitable for a particular application may be generated by chemical (Zarándi et al. 2007) or biotechnological methods (Scheibel et al. 2003). Once the fibrils are formed, they possess high stability under relatively harsh physical and chemical conditions. The global disorder in amyloid fibrillar arrangement, however, usually stands in the way of their widespread usability in nanotechnology applications. Recently, we have shown that amyloid β25–35 (Aβ25–35), a toxic fragment of Alzheimer's beta peptide, forms trigonally oriented fibrils on mica (Karsai et al. 2007). Oriented binding depends on an apparently cooperative interaction of a positively charged moiety on the Aβ25–35 peptide with the K^+-binding pocket of the mica lattice. The formation of oriented fibrils is the result of epitaxial polymerization, and the growth rate and the mesh size of the oriented amyloid fibril network can be tuned by varying the K^+ concentration. In principle, such a fibril network may be used in nanotechnology applications, provided that a specific chemical labeling of the fibrils is available. In the present

work, we explored the properties of a mutant Aβ25–35 peptide containing a Cys residue for the explicit purpose of specific chemical targeting. We find that the mutant Aβ25-35_N27C peptide, just like the wild-type peptide, forms trigonally oriented fibrils that develop, in a highly cation-sensitive manner, into a branched network. We show, by nanomechanical manipulation with a gold-coated AFM tip, that the sulfhydryl group of the Cys27 residue is oriented toward the solution and is chemically reactive, thus paving the way toward sophisticated nanotechnological utilization of amyloid fibrils.

Materials and methods

Sample preparation

N27C mutant Aβ25–35 (^{25}GSCKGAIIGLM^{35}-amide) peptide was produced by solid-state synthesis (Zarándi et al. 2007). The mutant peptide is hereby referred to as Aβ25–35_N27C. The lyophilized peptide was dissolved in DMSO (50.0 mg/ml) and diluted in 10 mM sodium phosphate buffer (10 mM Na_2HPO_4–NaH_2PO_4, pH 7.4, 20 mM DTT, 0.02% NaN_3) supplemented with different concentrations of KCl or NaCl. Insoluble aggregates were removed by high-speed centrifugation (Beckman Optima, 200,000$\times g$, 30 min). Final concentration ranged between 0.5 and 2 mg/ml. Peptide concentration was measured with the quantitative bicinchoninic acid assay (Smith et al. 1985). Aliquots of the sample were quick frozen in liquid nitrogen and stored at −80°C for further use. After thawing, the sample was diluted with buffer to a typical working concentration of 5 μM.

Atomic force microscopy

AFM measurements were carried out as described previously (Karsai et al. 2007). Typically, 100-μl samples were applied to freshly cleaved mica surface (V2 high-grade mica, #52-6, Ted Pella, Inc., Redding, CA). After 15-min incubation, the surface was washed gently with buffer to remove unbound fibrils. The samples were imaged with AFM in buffer under reducing conditions (20 mM DTT freshly added). Noncontact mode AFM images were acquired with an Asylum Research MFP3D instrument (Santa Barbara, CA) using silicon-nitride cantilevers (Olympus BioLever, typical resonance frequency in buffer 9 kHz). 512 × 512-pixel images were collected at a typical scanning frequency of 1 Hz and with a high set point (0.8–1 V). In binding assays, the amyloid sample was incubated on mica for 1 min in the presence of KCl or NaCl at increased, different concentrations. Subsequently, the surface was washed gently three times to remove the unbound fibrils. The AFM imaging was carried out in buffer. The relative fibril-covered surface area as a function of the KCl or NaCl concentration was measured. Time-lapse AFM images of Aβ25–35 fibril growth on mica were recorded by repetitively scanning 2–5 μm wide areas following the addition of the peptides. 512 × 512 pixel images were typically scanned at a rate of 3 Hz. Images were collected with no interleave pause. Surface-bound fibrils were mechanically manipulated by pressing the cantilever tip against a fibril, then pulling the cantilever away with a constant, preadjusted rate. Typical stretch rate was 500 nm/s. Nanomechanical experiments were carried out in buffer under oxidizing conditions (buffer without DTT).

Image processing and data analysis

AFM images were analyzed using algorithms built into the MFP3D driving software. Angles were measured manually between a line positioned in the fibril axis and a horizontal reference line. 2D FFT was carried out with the ImageJ program. For data analysis, we used IgorPro (Wavemetrics, Lake Oswego, OR).

Results and discussion

Binding and orientation of Aβ25-35_N27C fibrils on mica

Aβ25–35_N27C fibrils displayed a highly ordered trigonal arrangement on freshly cleaved mica surface (Fig. 1). The fibril orientation angles, relative to a horizontal reference line, were narrowly distributed around 20°, 80°, and 140° (Fig. 1e), thus revealing discrete, 60° differences between fibril orientations. The orientation angle distribution corresponds to an angle of 120° between each of three main fibril orientation directions. The regular fibril orientation was manifested in a hexagonal pattern in the two-dimensional fast Fourier transforms of the AFM images (Fig. 1b, c inset). Our observations are essentially identical to those obtained with the wild-type Aβ25–35 peptide (Karsai et al. 2007). Thus, the exchange of Gln27 to Cys did not interfere the orientation of fibrils on mica surface. The finding is consistent with our earlier conclusion that residues other than Gln27 contribute to the properties that define oriented binding to mica. The trigonal orientation of Aβ25–35_N27C fibrils is also consistent with the hexagonal crystalline lattice structure of the exposed mica surface (Brigatti et al. 2003; Franzini 1969; Giese 1979). The fibrils, just as their wild-type counterpart, thus follow one of the three main directions dictated by the hexagonal array of the surface lattice. Figure 1f shows the topographical height distribution along a linear section of the AFM image (Fig. 1c).

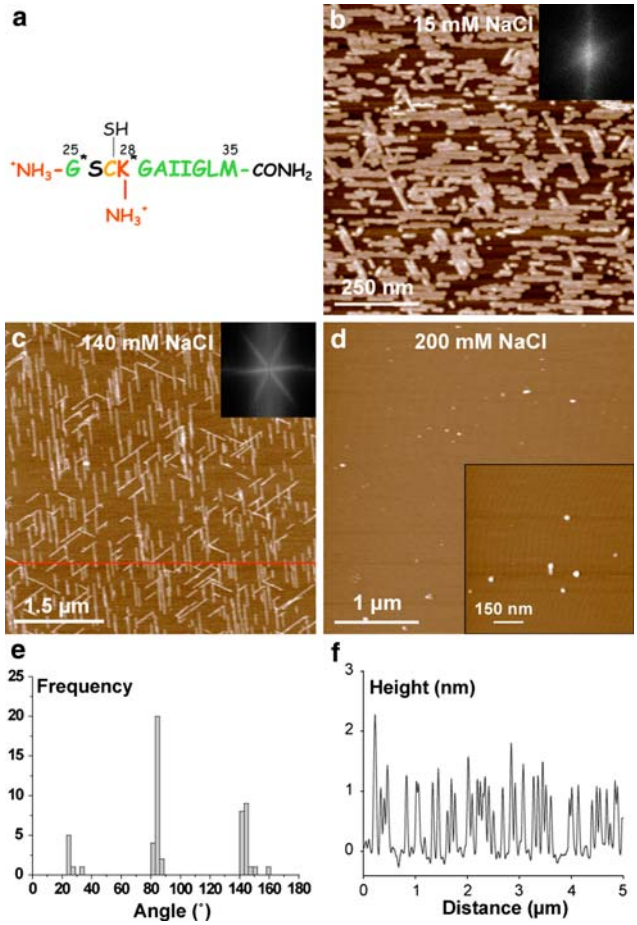

Fig. 1 **a** Schematic diagram of the Aβ25–35_N27C peptide. **b–d** AFM images of Aβ25–35_N27C fibrils bound to mica in presence of increasing concentrations of NaCl: 15 mM (**b**), 140 mM (**c**), and 200 mM (**d**); *Insets* **b** and **c** FFT of the corresponding AFM image; *Inset* **d** High-resolution image of Aβ25–35_N27C particles. **e** Distribution of orientation angles of Aβ25–35_N27C fibrils in **c**; reference axis (0°): horizontal. **f** Topographical height along a segment demarcated (in *red*) in **c**

The average height of the fibrils was 0.8 nm (±0.4, SD). This value most likely corresponds to the thickness of individual β-sheets formed of Aβ25-35_N27C peptides (Karsai et al. 2007).

Effect of cations on fibril binding

The binding of Aβ25–35_N27C to mica was sensitive to the presence of cations. We tested the effect of NaCl and KCl on fibril binding. Increasing NaCl concentration above 140 mM resulted in reduced binding of fibrils to the mica surface (Fig. 1). In the presence of 200 mM NaCl, only a few short fibrils and oligomers were observed (Fig. 1d). In contrast to our observations, fibrils composed of the wild-type peptide bound to mica at NaCl concentrations as large as 640 mM (Karsai et al. 2007). KCl-dependent binding experiments also revealed a weakened binding of Aβ25–35_N27C to mica (Fig. 2). Reduced binding of Aβ25–35_N27C fibrils was observed at KCl concentrations as low as 3 mM (Fig. 2b). The cutoff KCl concentration (KCl concentration at half-maximal relative fibril-covered area) was 18.4 mM in the case of the wild-type peptide, whereas in the case of Aβ25–35_N27C, it was only 4.6 mM. Thus, the N27C mutation, although did not affect fibril orientation, weakened the interaction with the mica surface. Our results indicate that fibril binding to mica is more sensitive to K^+ than to Na^+, although the effect is not as pronounced as in the case of the wild-type peptide. Most likely, the positively charged Lys28 side chain is coordinated by the K^+-binding pocket of the mica surface. Accordingly, the side chain of Cys27 is predicted to point away from the surface and be exposed to the solution (see Fig. 1a).

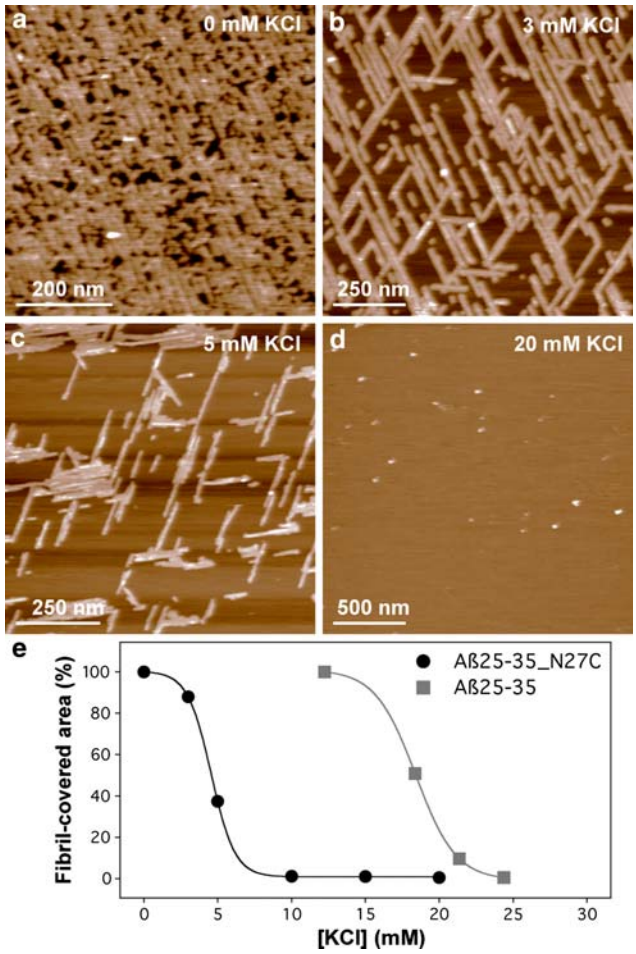

Fig. 2 AFM images of Aβ25–35_N27C fibrils bound to mica in presence of increasing concentrations of added KCl: 0 mM (**a**), 3 mM (**b**), 5 mM (**c**), and 20 mM (**d**). **e** Relative fibril-covered surface area as a function of KCl concentration. Hundred percent refers to the initial relative fibril-covered area

Temporal evolution of oriented Aβ25-35_N27C fibril network

The development of Aβ25–35_N27C orientation on mica was investigated in time-dependent experiments. Time-lapse AFM experiments showed that seeds appear on the mica surface from which fibrils grow in the main orientational directions (Fig. 3). Fibril growth proceeded until the fibril end reached a roadblock, typically in the form of another fibril lying across its path of growth. Once a growing fibril hit the side of an already developed fibril, its growth stopped (Fig. 3). We did not observe fibrils crossing over each other. In principle, individual, blocked fibrils could grow further by bending away from the roadblock. However, apparently such process does not take place, most likely because fibril growth depends on the structure of the mica surface lattice. Accordingly, the formation of oriented Aβ25–35_N27C fibrils involves epitaxial growth driven by mica. The process depends on peptide concentration and is modulated by the concentration of cations, which function as competitive inhibitors. K^+ is a more efficient competitor because of structural specificities of mica (Brigatti et al. 2003). Fibril growth involves an initial, cation-sensitive step of peptide binding to mica coordinated primarily by the interaction between mica's K^+-binding pocket and the ε-amino group of Lys28. Further binding of peptides to the initial fibril seed involves not only a direct interaction between mica and the peptide, but a hydrogen bonding between neighboring peptides as well. Because either set of bonds stabilizes the other type of interactions, mica-driven oriented Aβ25–35_N27C fibril growth proceeds with an apparent cooperativity faster than either the binding of peptides on the mica surface or the aggregation of fibrils in solution. Oriented fibril network is formed, in which the ends of individual fibrils form a contact with the side of another fibril. These contact points may be considered as branching points of the network. Interestingly, the network of Aβ25–25_N27C fibrils often displays directional preference. That is, one direction out of the three main orientations is more populated. Such a scenario can be seen in Fig. 3, where the majority of fibrils run between the top and bottom of the field of view. The molecular basis of the directional preference is yet to be investigated.

Nanomechanical probing of Aβ25-35_N27C fibrils

Because of the expected structure of the Aβ25–35_N27C peptide (Fig. 1a), the dimensions of the fibrils (Fig. 1f), and the interactions responsible for their binding to mica, it is predicted that the sulfhydryl group of Cys27 is exposed to the buffer solution. To test this hypothesis, we probed the surface of the fibrils with a gold-coated AFM cantilever tip under oxidizing conditions. The cantilever tip was pressed against a fibril at predetermined locations, then pulled away with a preadjusted velocity. Subsequently, the surface was scanned to investigate the effect of the mechanical perturbation. The results are shown in Fig. 4. The local nanomechanical manipulation of the Aβ25–35_N27C fibrils resulted in the removal of small fibril fragments (Fig. 4b). This is in striking contrast to our previous observations on Aβ1–40 (Kellermayer et al. 2005), Aβ1–42 (Karsai et al. 2006), and wild-type Aβ25–35 fibrils (Karsai et al. 2007). The results indicate that the energy of the bonds formed between the tip and the peptide exceed that of the bonds holding the fibril together. The most plausible explanation is that a covalent bond has formed between Au atoms on the cantilever tip and the S atom of Cys27. It has been shown that both cysteine and methionine interact with colloidal gold through the S atom of the residue (Podstawka et al. 2005). Therefore, Met35 of the Aβ25–35 peptide might also contribute to our observations. However, the thiol group of Cys interacts with gold much more strongly than the $-S-CH_3$ group of methionine (Podstawka et al. 2005). Furthermore, Met35 is present in the wild-type peptide, in the case of which the removal of fibril segments was not observed. Thus, it is more likely that during scanning, the Au–Cys27 rather than the Au–Met35 interaction results in the removal of fibril segments. Our observations suggest that the sulfhydryl group of Cys27 is indeed in an exposed position within the oriented fibril network. Notably, there does not seem to be a difference between the end or the middle of a fibril in its reactivity with the Au-coated AFM tip (Fig. 4). Thus, Aβ25–35_N27C fibrils seen in our AFM images most likely correspond to β-sheets lying flat on the mica surface.

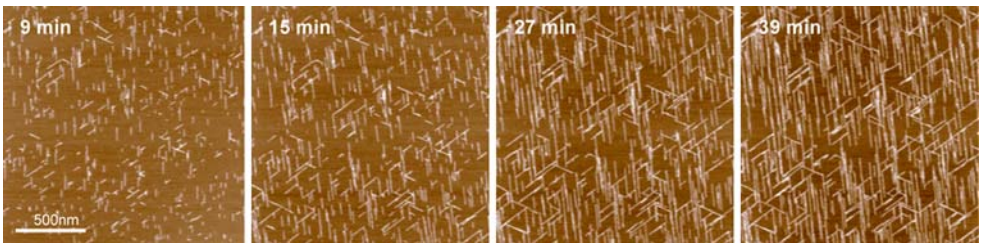

Fig. 3 In situ time-lapse AFM of oriented Aβ25–35_N27C fibril growth in the presence of 140 mM NaCl. Time stamps indicate the time elapsed from the beginning of sample incubation to the end of the respective AFM scan

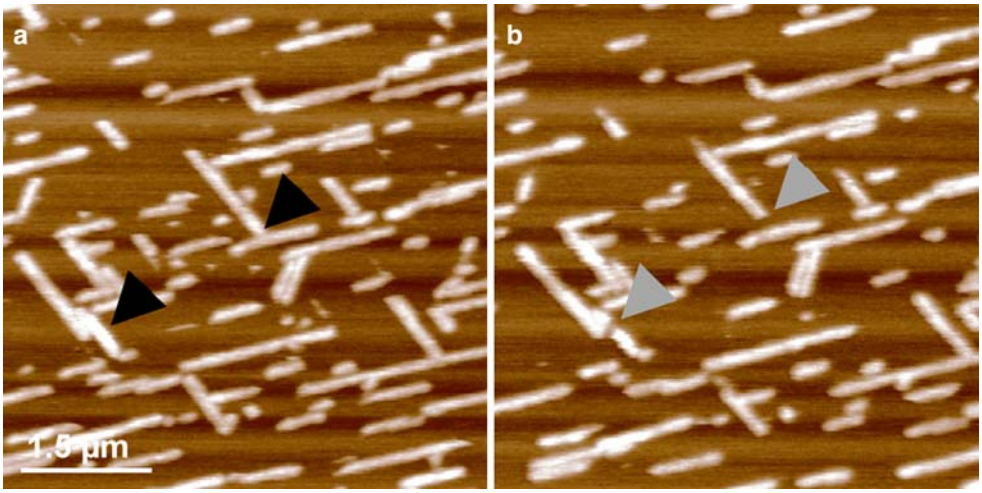

Fig. 4 In situ nanomechanical manipulation of mica-associated Aβ25–35_N27C fibrils. **a** AFM image of fibrils prior to nanomechanical manipulation. *Black arrowheads* point at the target points of manipulation. **b** AFM image obtained following nanomechanical manipulation. *Gray arrowheads* point at the manipulated sites, where fibril discontinuity can be discerned

Conclusions and perspectives

In the present work, we demonstrated that the N27C mutant of Aβ25–35 peptide forms a trigonally oriented fibril network on mica, similar to its wild-type counterpart. The binding and growth of the fibrils, hence the development of the surface network, depends on cation concentration. The cation-dependence of amyloid fibril growth may be used to fine-tune the properties of the network (e.g., average fibril length, number of branching points). We have shown that the sulfhydryl group of Cys27 is oriented toward the solution along the fibril's length, and is chemically accessible and reactive. By specifically labeling the Cys27 side chain, Aβ25–35_N27C amyloid fibrils may be utilized in the construction of regular arrays of biomolecular nanostructures such as nanomechanical devices (by attaching motor proteins), nanosensors (by using enzymes), or nanoelectrical circuits (by attaching nanogold particles).

Acknowledgments This work was supported by grants from the Hungarian Science Foundation (OTKA T049591, IN70320, and TS 049817), Hungarian National Office for Research and Technology (OMFB-01600/2006, OMFB-01627/2006, OMFB-00198/2007, OMFB-00785/2007, KFKT-1-2006-0021, RET 08/2004), and the Hungarian Ministry of Health (ETT-506/2006).

References

Brigatti MF, Guggenheim S, Poppi M (2003) Crystal chemistry of the 1M mica polytype: the octahedral sheet. Am Mineral 88:667–675

Franzini M (1969) The A and B mica layers and the crystal structure of sheet silicates. Contrib Mineral Petrol 21:203–224

Gazit E (2006) Use of biomolecular templates for the fabrication of metal nanowires. FEBS J 274:317–322

Giese RFJ (1979) Hydroxyl orientations in 2:1 phyllosilicates. Clays Clay Miner 27:213–223

Hamada D, Yanagihara I, Tsumote K (2004) Engineering amyloidogenicity towards the development of nanofibrillar materials. Trends Biotechnol 22:93–97

Hardy J, Selkoe DJ (2002) The amyloid hypothesis of Alzheimer's disease: progress and problems on the road to therapeutics. Science 297:353–356

Karsai Á, Grama L, Murvai Ü, Soós K, Penke B, Kellermayer MSZ (2007) Potassium-dependent oriented growth of amyloid β25–35 fibrils on mica. Nanotechnology 18:345102

Karsai Á, Mártonfalvi Z, Nagy A, Grama L, Penke B, Kellermayer MSZ (2006) Mechanical manipulation of Alzheimer's amyloid β1–42 fibrils. J Struct Biol 155:316–326

Kellermayer MS, Grama L, Karsai A, Nagy A, Kahn A, Datki ZL, Penke B (2005) Reversible mechanical unzipping of amyloid beta-fibrils. J Biol Chem 280:8464–8470

Podstawka E, Ozaki Y, Proniewicz LM (2005) Surface-enhanced Raman scattering of amino acids and their homopeptide monolayers deposited onto colloidal gold surface. Appl Spectrosc 59:1516–1526

Reches M, Gazit E (2003) Casting metal nanowires within discrete self-assembled peptide nanotubes. Science 300:635–627

Scheibel T, Parthasarathy R, Sawicki G, Lin XM, Jaeger H, Lindquist SL (2003) Conducting nanowires built by controlled self-assembly of amyloid fibers and selective metal deposition. Proc Natl Acad Sci USA 100:4527–4532

Selkoe DJ (2001) Alzheimer's disease: genes, proteins and therapy. Physiol Rev 81:741–766

Selkoe DJ (2003) Folding proteins in fatal ways. Nature 426:900–904

Serpell LC (2000) Alzheimer's amyloid fibrils: structure and assembly. Biochim Biophys Acta 1502:16–30

Smith PK, Krohn RI, Hermanson GT, Mallia AK, Gartner FH, Provenzano MD, Fujimoto EK, Goeke NM, Olson BJ, Klenk DC (1985) Measurement of protein using bicinchoninic acid. Anal Biochem 150:76–85

Zarándi M, Soós K, Fülöp L, Bozsó Z, Datki Z, Tóth GK, Penke B (2007) Synthesis of Aβ(1–42) and its derivatives with improved efficiency. J Pept Sci 13:94–99